

# Thermal Analysis of Cellulose Treated with Boric Acid or Ammonium Phosphate\* in Varied Oxygen Atmospheres

TOSHIMI HIRATA,\*\* *Forestry and Forest Products Research Institute, P. O. Box 16, Tsukuba Norin Kenkyu, Danchi-Nai, Ibaraki, 305 Japan* and KATHLEEN E. WERNER, *Department of Chemistry, University of California at Santa Barbara, Santa Barbara, California 93106*

## Synopsis

Thermal analyses (TG, DTG, and DSC) of cellulose treated with diammonium phosphate or boric acid were conducted in atmospheres of differing oxygen concentration ( $N_2$ , and 2.5, 10, 21%  $O_2$  in He). The weight loss process from both untreated and treated cellulose consists of a first, slow stage, a second, rapid stage, and a third, prolonged, char oxidation stage. The first two stages appear to be first-order reactions; their Arrhenius parameters were obtained. Both of the additives accelerate the beginning of the weight loss, increase the char yield, and inhibit the char oxidation. Boric acid inhibits the first stage and ammonium phosphate promotes it. The effects of oxygen are smaller than those of the additives. Oxygen produces three effects: acceleration of the beginning of the weight loss, an increase in the char yield, and oxidative gasification of the char. However, the dominant of these three effects changes depending on the oxygen concentration. The main weight loss and the char yield for untreated and treated cellulose may be explained by a chain reaction consisting of random-scission initiation, depropagation producing levoglucosan, and grafting termination, all describable by Arrhenius kinetics.

## INTRODUCTION

An enormous amount of research on the thermal degradation of cellulosic materials has been reported. This has largely been concerned with flame retardation and, recently, with biomass energy production and chemical conversion. There is confusion as to the proper kinetic parameters of the pyrolysis; several kinetic models<sup>1-5</sup> have been proposed in attempts to resolve this. These attempts seem, however, to have been largely unsuccessful. The pyrolysis mechanism, which is accepted to be a chain reaction polymer degradation in the solid state, is very complex and variable. Evidently the complexities arise because, among other things, the activated centers of the reaction are very sensitive to the fine structure of the cellulose and its impurities; retardant chemicals also have a major impact, presumably for similar reasons. The yields of primary pyrolysis products differ depending on these details. The mode of action of fire retardants is thus intimately intertwined with the pyrolysis process. In seeking better retardants we must examine this interaction. The presence of oxygen adds more complications;

\*Contribution from the National Bureau of Standards, not subject to copyright

\*\*Guest worker from Forestry and Forest Products Research Institute, Tsukuba, 305, Japan, and to whom all correspondence should be addressed.

therefore, most studies have been conducted in inert atmospheres. The thermal decomposition of cellulose is promoted by oxygen.<sup>6-10</sup> The activation energy for chain scission is reportedly reduced in air relative to that in an inert atmosphere. For weight loss, however, the activation energy has been reported both to be reduced,<sup>6-8</sup> and to be increased.<sup>7,8</sup> It is desirable to clear up this confusion as to the effect of oxygen on the activation energy for weight loss. Furthermore, the combustion of cellulosic materials in fires, particularly in smoldering fires, proceeds over a range of ambient oxygen concentrations. Thus, the effects of oxygen concentration on the pyrolysis and its kinetic description need to be determined as an aid in developing quantitative understanding of the combustion of cellulosic materials.

This paper deals with two of the complicating factors in combination. It reports a study, using thermal analysis, of cellulose treated with representative inorganic flame retardants in environments of differing oxygen concentration and describes the effects of both oxygen concentration and the flame retardants on pyrolysis.

## EXPERIMENTAL

### Materials

The cellulose used was a purified fibrous cotton linter. The flame retardants used to treat the cellulose were reagent-grade boric acid and diammonium hydrogen phosphate. The cellulose sample was first immersed in an aqueous solution of one of the flame retardants for about one hour. The cellulose sample was recovered by first filtering the suspension through a porous glass funnel and then freeze drying the solid. The flame-retardant solutions were prepared in levels from 0.5 to 3.0% by weight. The average mass percentages of boric acid in the cellulose samples were 0.3, 3.4, and 9.3% of the original cellulose weight; those of ammonium phosphate were 2.0, 4.8, and 10.0%. All cellulose samples were conditioned in a vacuum desiccator before thermal analysis.

### Thermal Analyses

Each cellulose sample of 4 to 5 mg weight was placed in a covered, gold-coated aluminum oxide crucible for simultaneous thermogravimetric (TG) and differential scanning calorimetric (DSC) measurements at 5°C/min in a Mettler TA2000C thermoanalyzer.\* Four different atmospheres, pure nitrogen, 2.48, 10.1, and 20.95 O<sub>2</sub> in helium, were used; helium was used in the presence of oxygen to enhance oxygen diffusion into the porous solid phase. A flow of about 25 mL/min of the test gas passed continuously around the sample crucible in the furnace. Before the test, the thermoanalyzer system dead volume was subjected to repeated cycles of evacuation and filling to atmospheric pressure with the test gas to remove all traces of air.

\*Certain commercial equipment, instruments, or materials are identified in this paper in order to adequately specify the experimental procedure. Such identification does not imply recommendation or endorsement by the National Bureau of Standards, nor does it imply that the materials or equipment identified are necessarily the best available for the purpose.

The weight and the temperature of the sample, the DSC heat flow, and the time were simultaneously recorded by a computer. At first, a baseline run with empty cells was conducted, and then a sample run was repeated for each condition. The actual weight and DSC heat flow were calculated from the difference between the sample and baseline runs. This procedure minimized the artificial effects of the temperature elevation on the heat capacity of the cells and buoyancy, which affect the apparent TG and DSC values; however, some DSC baseline problems remained. Derivative thermogravimetry (DTG) plots were obtained after the tests by numerical differentiation and smoothing of the TG data to remove the inevitable noise that differentiation produces.

## RESULTS

### Thermal Analyses of Cellulose Treated with Ammonium Phosphate

In the pyrolysis of the cellulose samples in nitrogen, the beginning of the weight loss was accelerated and the char yield increased as a result of the treatment by ammonium phosphate, as shown in Figure 1. Also it is seen that the maximum weight loss rate, namely, the peak height in the DTG curves, and the peak temperature decreased with an increase in the salt content. The peaks have shoulders on the low temperature side which become clearer with increasing salt content. The overall weight loss is divided into at least three different stages, the first, slow weight loss represented by the shoulder, the second, rapid stage, and then the prolonged decomposition of the char.

Although the maximum DSC heat flow was reduced by the salt, the heat effect of the first two weight loss stages can be discerned in the DSC curves of Figure 2. Two endotherms, designated a and b in the figure, appear to correspond to these two stages. The temperatures at a and b agree with those

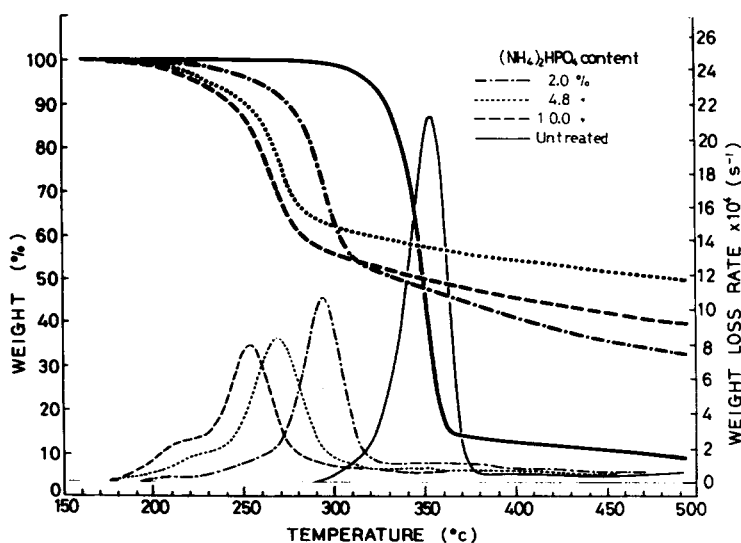


Fig. 1. TG and DTG curves in  $N_2$  of cellulose treated with ammonium phosphate.

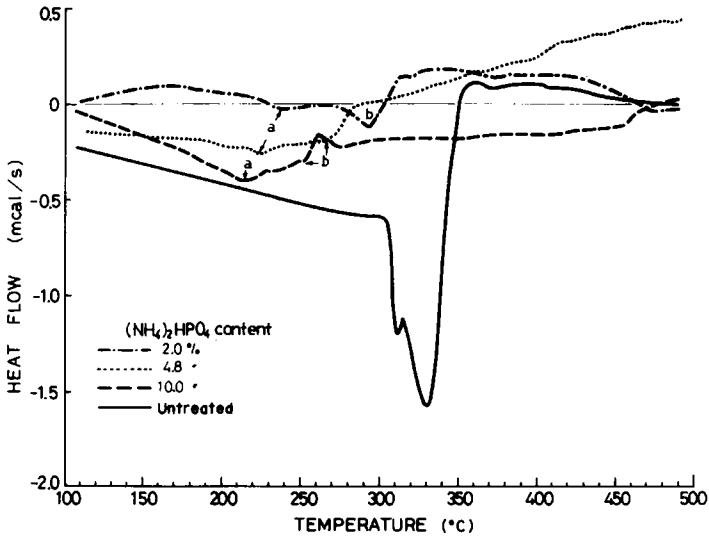


Fig. 2. DSC curves in  $N_2$  of cellulose treated with ammonium phosphate.

at the DTG shoulders and peaks. It appears that endotherm *a* becomes deeper and endotherm *b* becomes shallower with increasing salt content.

Also, in pyrolyses in the presence of oxygen, the threshold temperature for weight loss was lowered and the char yield increased with an increase in the salt content, as shown in Figures 3 and 4. Similarly to that in nitrogen, the weight loss consists of three different stages, as seen in Figure 5.

The DSC curves for the 2.5%  $O_2$  atmosphere show an endothermic and an exothermic peak for each sample, as seen in Figure 3. (Note the general downward shift of the DSC baseline here.) These peaks become broader as the

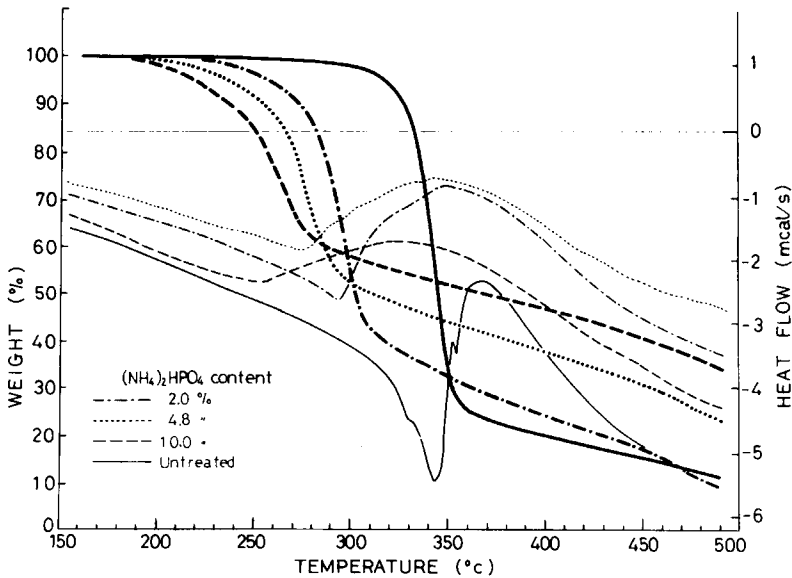


Fig. 3. TG and DSC curves in 2.5%  $O_2$  of cellulose treated with ammonium phosphate.

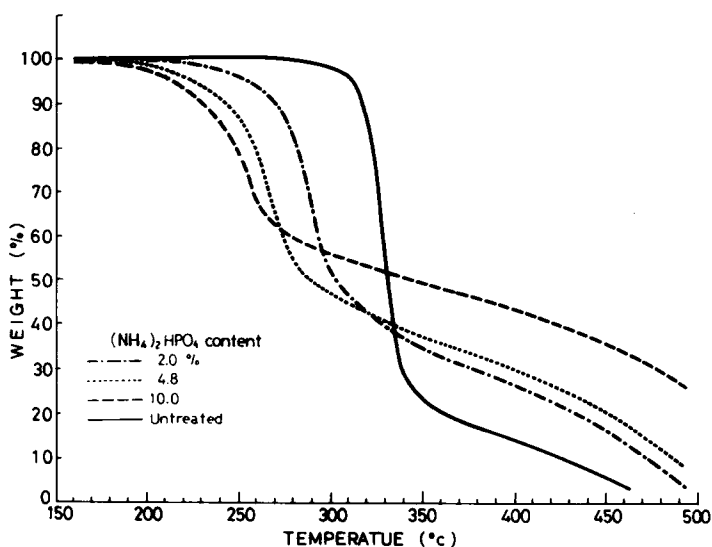


Fig. 4. TG curves in 21%  $O_2$  of cellulose treated with ammonium phosphate.

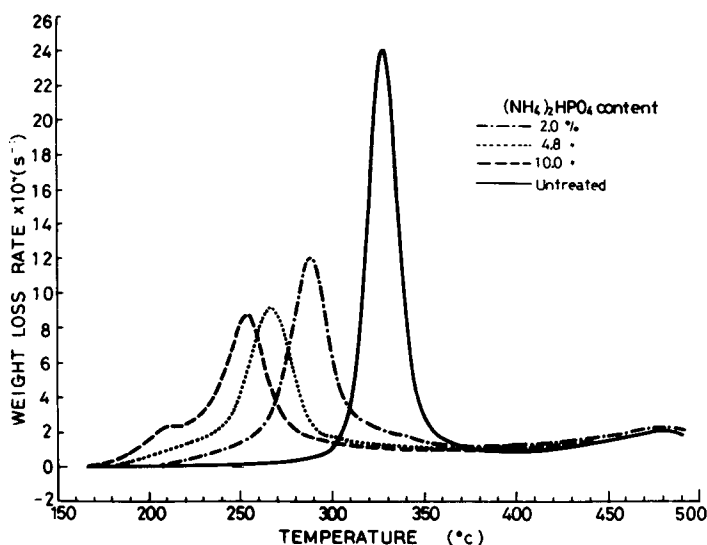


Fig. 5. DTG curves in 21%  $O_2$  of cellulose treated with ammonium phosphate.

salt content increases. The endothermic peaks corresponding to the active weight loss presumably are mainly attributable to evaporation of the pyrolysis products and the exothermic peaks to oxidation of the charred solid residue, as suggested by comparison between the TG and DSC curves. The endotherm is gradually overwhelmed by the exotherm with increasing ambient oxygen concentration. In 10%  $O_2$  endothermic evaporation is possibly responsible for the small dip on the leading edge of the exothermic peaks, as shown in Figure 6. This endothermic effect, however, is completely covered by the oxidation of the char in the 21% oxygen atmosphere, as shown in Figure 7.

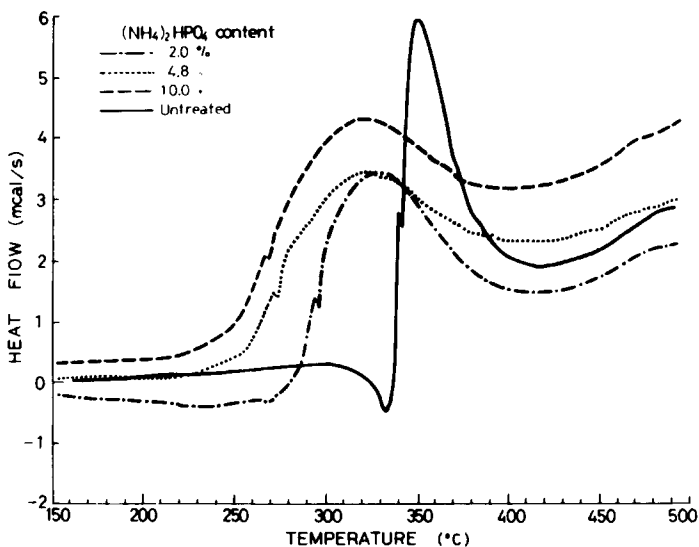


Fig. 6. DSC curves in 10%  $\text{O}_2$  of cellulose treated with ammonium phosphate.

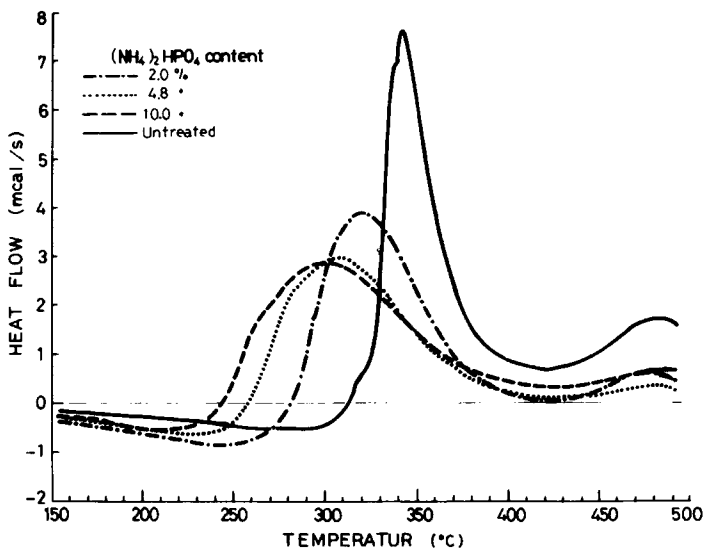


Fig. 7. DSC curves in 21%  $\text{O}_2$  of cellulose treated with ammonium phosphate.

This suggests that the degradation process produces primary volatiles such as levoglucosan and water, and forms an oxidizable residue at the same time.

The temperatures corresponding to the DTG peak for the second, rapid weight loss stage drop sharply with the first few percent of added ammonium phosphate, as shown in Figure 8. Also the DTG peak heights are reduced by this salt, as shown in Figure 9. Thus ammonium phosphate accelerates the onset of the rapid weight loss stage but lowers its peak rate. However, oxygen has a different effect. It is seen from Figures 8 and 9 that, for the untreated cellulose, higher oxygen concentration lowers the temperature of the DTG peak, but raises the corresponding DTG peak height. A similar relation is seen

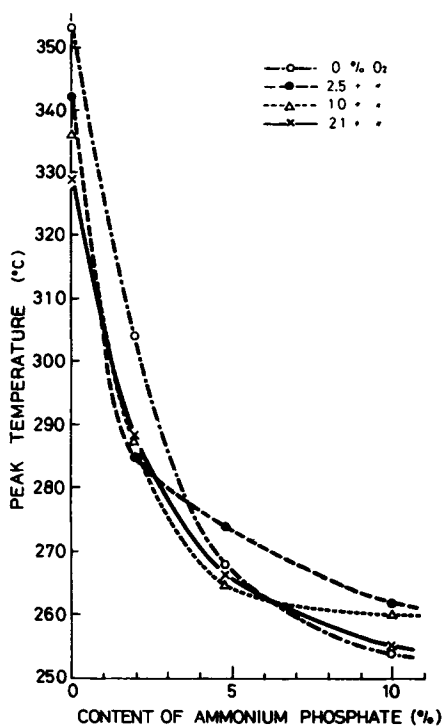


Fig. 8. Changes in the DTG peak temperature in different atmospheres with ammonium phosphate content.

for 2% salt content. It is difficult to discern any definite trend of oxygen influence at higher salt contents, probably because of competing effects between ammonium phosphate and oxygen on the pyrolysis. This problem will be discussed later.

The temperatures of the DSC peaks corresponding to the second, rapid weight loss stage are shown in Figure 10 as a function of salt content; depending on the oxygen level this peak may be endothermic or exothermic, as seen before. The downward trend with increasing salt content agrees with the accelerated onset of the active weight loss due to the salt.

### Thermal Analyses of Cellulose Treated with Boric Acid

In TG of cellulose in nitrogen, the onset of weight loss is accelerated by boric acid, as shown in Figures 11 and 12. However, the onset temperatures for the rapid weight loss stage from the treated samples are almost independent of the amount of boric acid added. Another boron compound, sodium tetraborate shows a similar effect.<sup>11</sup> The char yield from the rapid weight loss stage increases with boric acid content. The rapid weight loss stage of the treated samples occurs abruptly, agreeing with previous results for cellulose treated with this acid;<sup>12</sup> the DTG curves do not have shoulders on the low temperature side, as shown above for the samples treated with ammonium phosphate. The DSC curves in nitrogen show sharp endothermic peaks coincident with the rapid weight loss, as seen in Figure 13. After this endotherm only the

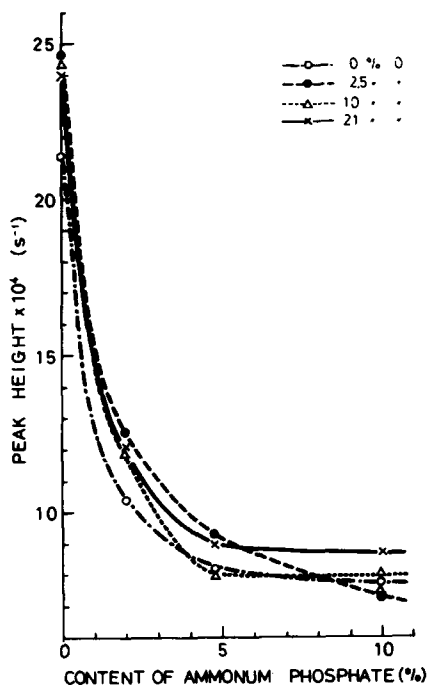


Fig. 9. Changes in the DTG peak heights in different atmospheres with ammonium phosphate content.

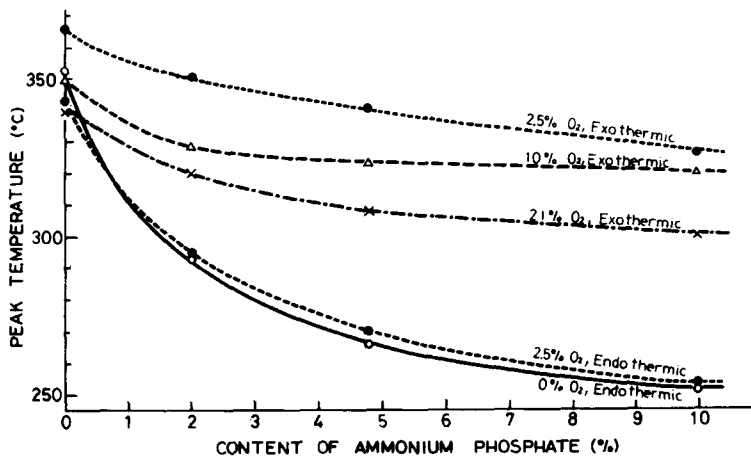


Fig. 10. Dependency of the DSC peaks in different atmospheres on ammonium phosphate content.

sample with the highest chemical content gave an apparent exothermic peak, but again the exact position of the DSC baseline is uncertain. A similar exothermic peak has been previously observed in differential thermal analysis (DTA) curves (under vacuum) of cellulose treated with sodium tetraborate.<sup>13</sup>

In oxidizing atmospheres, the TG and DTG behavior of the treated samples is basically similar to that in nitrogen, as shown in Figures 14–16. However,



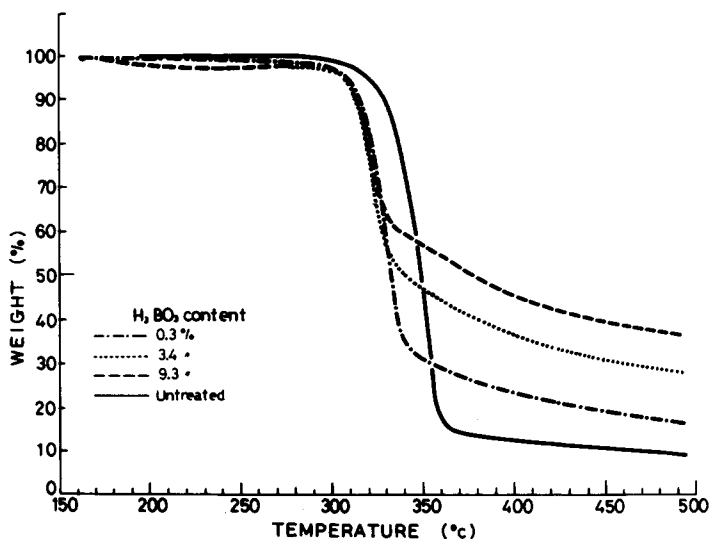


Fig. 11. TG curves in  $N_2$  of cellulose treated with boric acid.

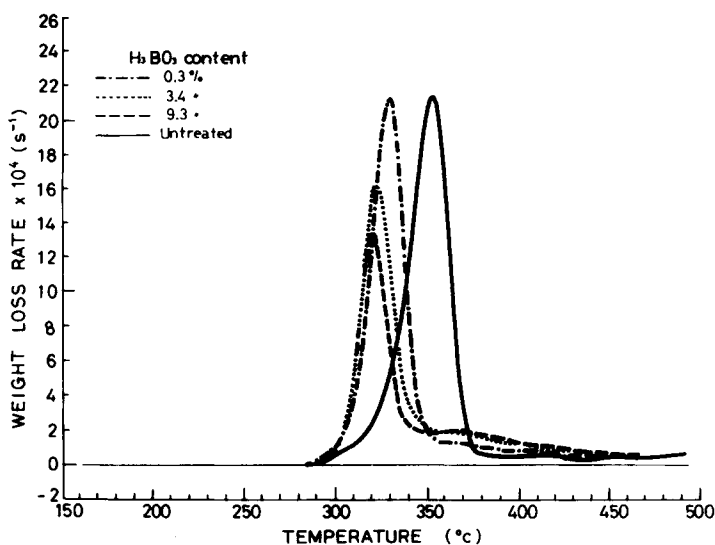


Fig. 12. DTG curves in  $N_2$  of cellulose treated with boric acid.

the DSC curves yield strong exotherms after the initial endothermic peaks accompanying the rapid weight loss stage, as shown in Figure 14 for 2.5%  $O_2$ . These exotherms are evidently caused by the oxidation of the charred residue, as is inferred from comparison of the TG and DSC curves. These exotherms become stronger with increasing oxygen concentration and completely overcome the initial endotherm at the highest oxygen concentration, as shown in Figures 17 and 18. The observed competition between the endotherm and the exotherm again implies that the rapid weight loss stage simultaneously yields volatile products and a char; this interpretation is the basis of a pyrolysis model by Bradbury and others<sup>5</sup> by Shafizadeh and others.<sup>14</sup>

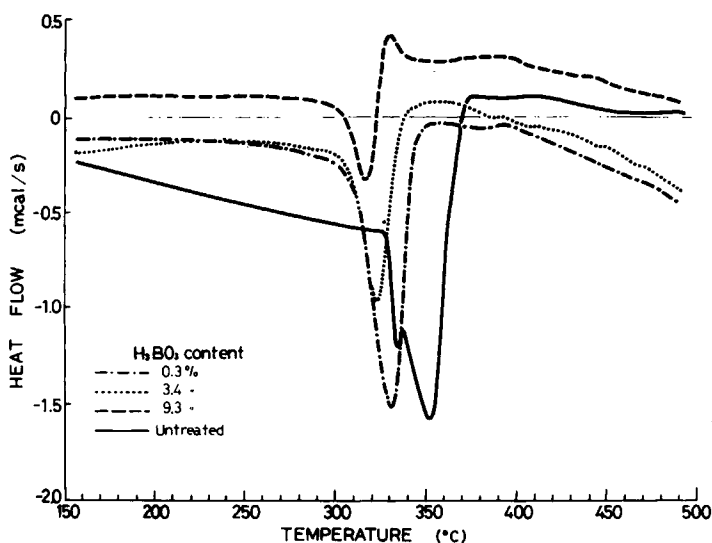


Fig. 13. DSC curves in N<sub>2</sub> of cellulose treated with boric acid.

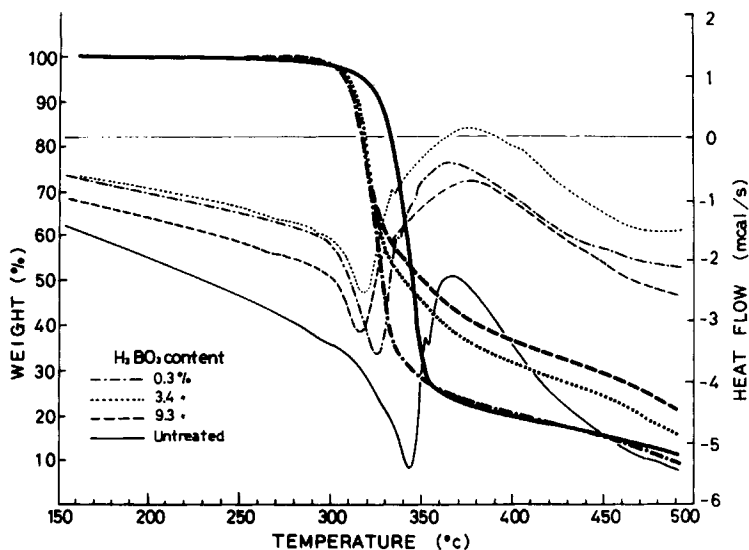


Fig. 14. TG and DSC curves in 2.5% O<sub>2</sub> of cellulose treated with boric acid.

In 10% or more O<sub>2</sub> the DSC curves show a second exothermic region at a temperature higher than 450°C, as seen in Figures 17 and 18. Similar indications of a second exotherm can be found for the samples treated with ammonium phosphate, as shown in Figures 6 and 7. Sekiguchi and Shafizadeh<sup>15</sup> found two exothermic peaks in the DSC curves (in air) of a partially pyrolyzed cellulose. According to them, the present second exotherm can be ascribed to oxidation of aromatic components of the charred residue and the first sharp exotherm is due to unstable aliphatic groups in the degraded solid. The relatively accelerated weight loss of char corresponding to the second DSC

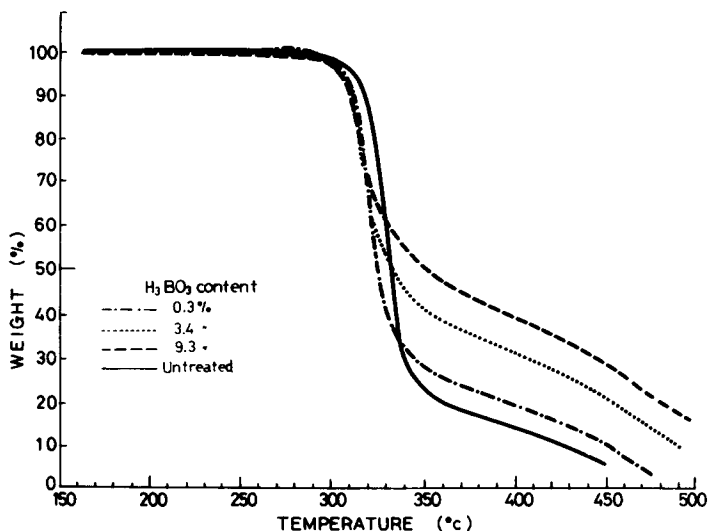


Fig. 15. TG curves in 21%  $O_2$  of cellulose treated with boric acid.

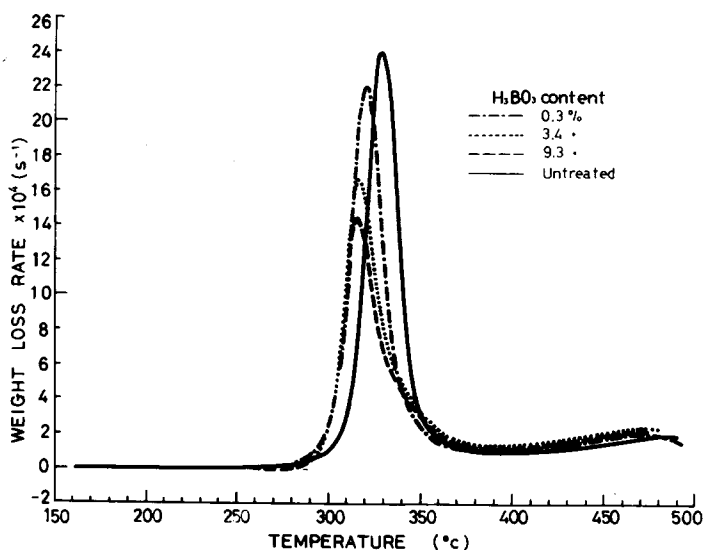


Fig. 16. DTG curves in 21%  $O_2$  of cellulose treated with boric acid.

exotherm can be found in the TG and DTG curves in the higher temperature range of Figures 4, 5, 15, and 16.

The DTG peaks shift substantially toward a lower temperature with an increase from 0 to 0.3% in boric acid content but the shifts are very small with further increases in the acid as shown in Figure 19. This DTG behavior is much different from that for cellulose treated with ammonium phosphate: there, at any fixed salt content, the DTG peak temperature decreased with an increase in the ambient oxygen concentration, but the DTG peak heights were reduced with increased salt content. Also, with ammonium phosphate, the impact of oxygen on the DSC peak heights varied with the salt content.

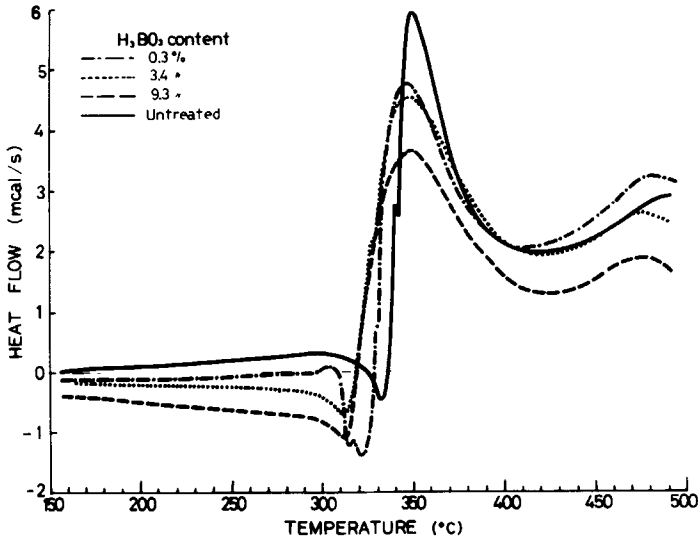


Fig. 17. DSC curves in 10% O<sub>2</sub> of cellulose treated with boric acid.

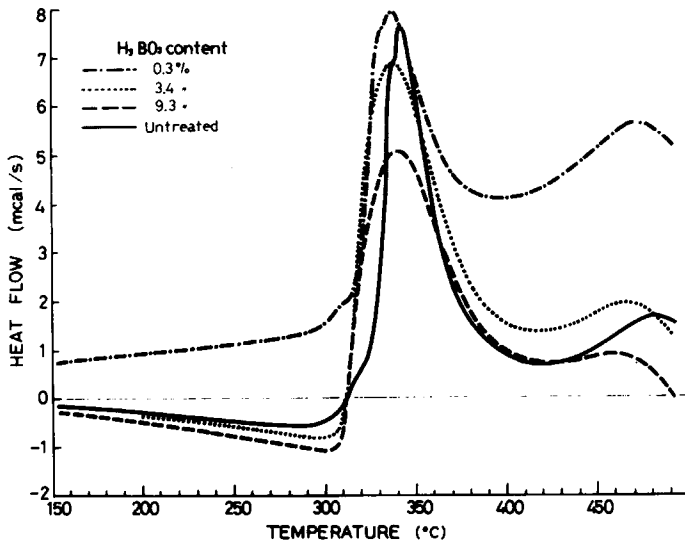


Fig. 18. DSC curves in 21% O<sub>2</sub> of cellulose treated with boric acid.

Returning to the effect of boric acid, one finds that the temperature of the DSC endothermic peaks is lowered with an increase in the chemical content as well as with an increase in the oxygen concentration, as shown in Figure 20. This parallels the DTG peak behavior. The temperature of the first strong exothermic peak is reduced with an increase of 0 to 0.3% in the boric acid content, but higher levels reverse the trend, in contrast to the effect of ammonium phosphate. The peak temperature of the same exotherm decreases

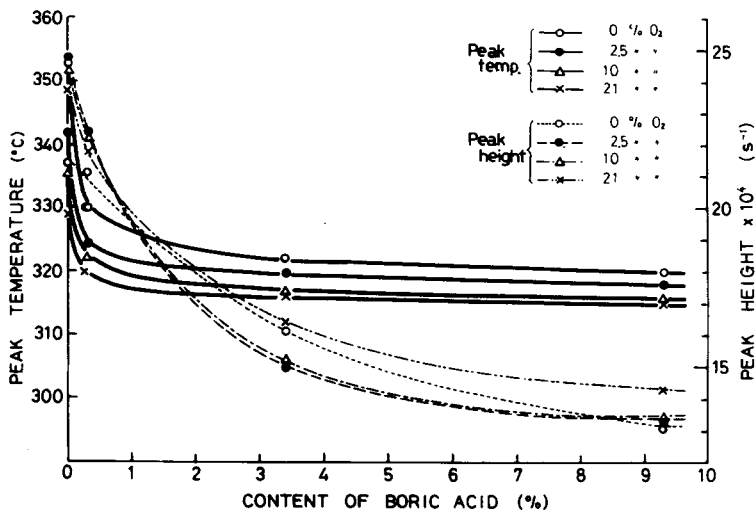


Fig. 19. Dependency of the DTG peak temperature and height in different atmospheres on boric acid content.

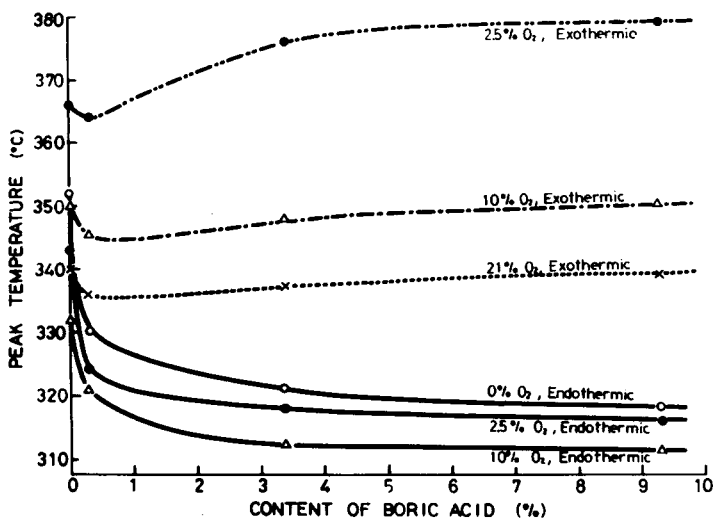


Fig. 20. Dependency of the DSC peak temperatures in different atmospheres on boric acid content.

with an increase in the oxygen concentration as the char oxidation rate accelerates.

### Kinetics

The weight loss from cellulose due to its thermal decomposition has been empirically shown by many researchers to obey first-order kinetics with respect to the remaining weight of the fuel.<sup>16</sup> Therefore, the Arrhenius parameters of the weight loss were determined in this study on the basis of an apparent first-order reaction. The weight loss rate in a first-order reaction is

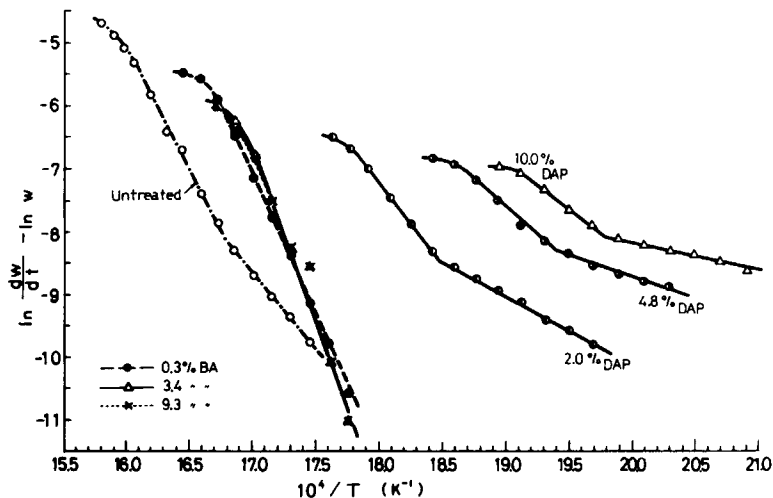


Fig. 21. Arrhenius plots for first-order weight loss in  $N_2$  of cellulose treated with boric acid (BA) and ammonium phosphate (DAP).

expressed as

$$\frac{dw}{dt} = -kw \quad (1)$$

where  $w$  is the weight,  $t$  the time, and  $k$  the rate constant. Since the temperature is a function of time, Eq. (1) reduces to

$$\ln\left(-\frac{dw}{dt}\right) - \ln w = \ln A - E/RT \quad (2)$$

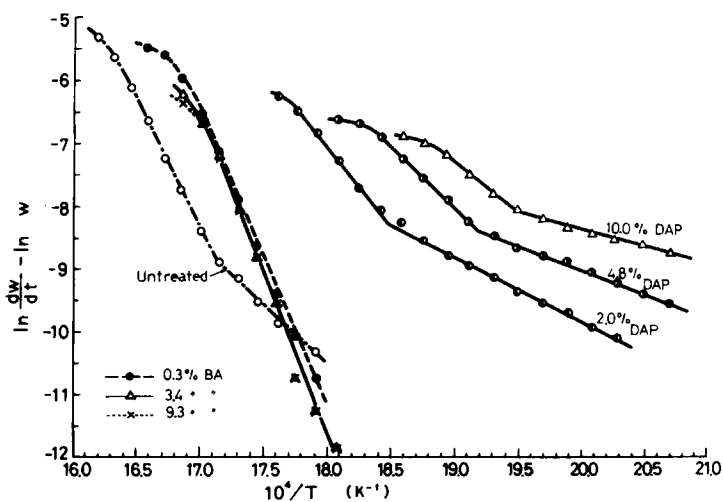


Fig. 22. Arrhenius plots for first-order weight loss in 2.5%  $O_2$  of cellulose treated with boric acid and ammonium phosphate.

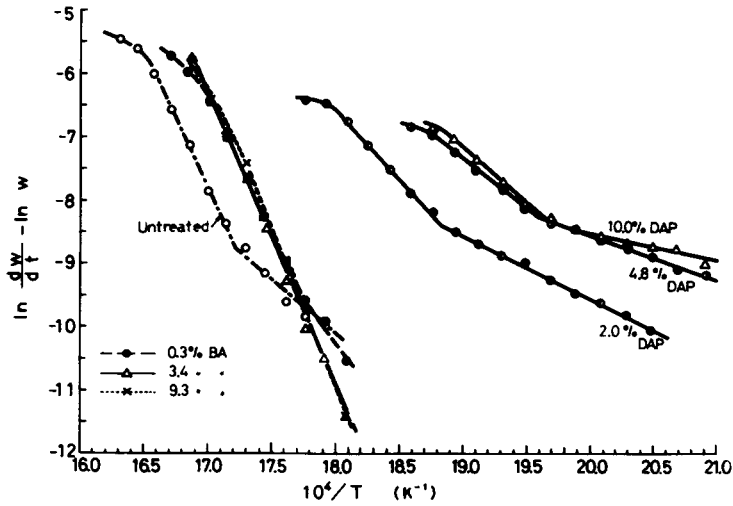


Fig. 23. Arrhenius plots for first-order weight loss in 10%  $O_2$  of cellulose treated with boric acid and ammonium phosphate.

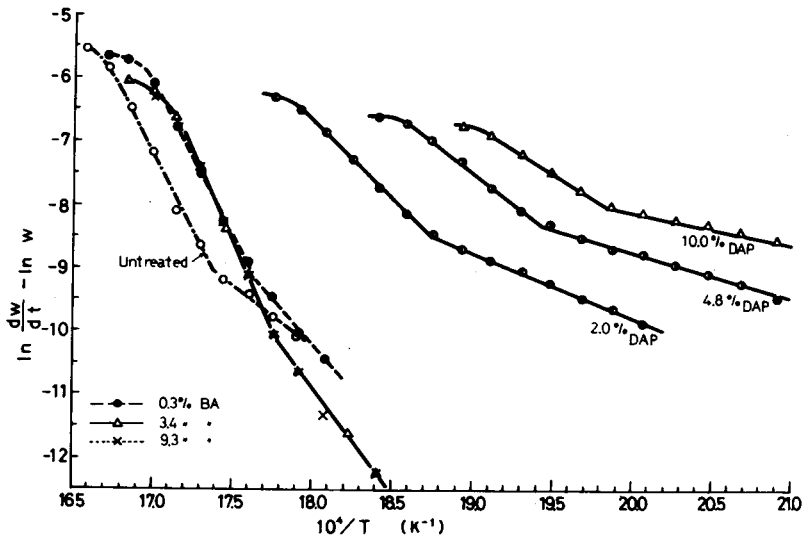


Fig. 24. Arrhenius plots for first-order weight loss in 21%  $O_2$  of cellulose treated with boric acid and ammonium phosphate.

where  $A$  and  $E$  are the Arrhenius pre-exponential factor and activation energy, respectively,  $R$  is the gas constant, and  $T$  is the temperature. Therefore, plots of the left-hand side of Eq. (2) against  $(1/T)$  provide the apparent Arrhenius parameters.

These plots, derived from the TG and DTG curves, are shown in Figures 21–24. The plots yield two (or sometimes one) straight line sections, usually one with a steep slope in the high temperature region and one with a lesser slope in the low temperature region. (There are two exceptions in Figure 22: the samples treated with boric acid in an atmosphere of nitrogen or 2.5%  $O_2$  in He.) At the high temperature end these plots curve back toward a lesser slope.

TABLE I  
 Arrhenius Parameters of Weight Loss in Different Atmospheres

Treatment	Stage O <sub>2</sub> %	E(kJ/mole)				A (s <sup>-1</sup> )			
		0	2.5	10	21	0	2.5	10	21
Untreated	First	206	164	143	149	$3.6 \times 10^{14}$	$6.6 \times 10^{10}$	$1.1 \times 10^9$	$3.8 \times 10^9$
	Second	310	328	348	397	$4.7 \times 10^{23}$	$3.1 \times 10^{25}$	$1.2 \times 10^{27}$	$1.5 \times 10^{32}$
2 % DAP	First	93	83	81	86	$2.1 \times 10^5$	$2.7 \times 10^4$	$2.3 \times 10^4$	$5.1 \times 10^4$
	Second	214	205	180	206	$1.1 \times 10^{17}$	$1.8 \times 10^{16}$	$1.2 \times 10^{14}$	$3.1 \times 10^{16}$
4.8 % DAP	First	60	66	60	59	$3.0 \times 10^2$	$1.1 \times 10^3$	$3.4 \times 10^2$	$2.4 \times 10^2$
	Second	150	159	135	167	$3.5 \times 10^{11}$	$2.0 \times 10^{12}$	$1.5 \times 10^{10}$	$2.3 \times 10^{13}$
10 % DAP	First	38	39	36	42	2.8	2.8	1.1	8.5
	Second	135	123	137	125	$2.6 \times 10^{10}$	$1.1 \times 10^9$	$3.2 \times 10^{10}$	$2.8 \times 10^9$
0.3 % BA	First			213	249			$3.7 \times 10^{15}$	$1.1 \times 10^{19}$
	Second	357	392	364	411	$4.7 \times 10^{28}$	$9.2 \times 10^{31}$	$3.9 \times 10^{29}$	$7.3 \times 10^{33}$
3.4 % BA	First				273				$1.1 \times 10^{21}$
	Second	417	435	405	497	$1.3 \times 10^{34}$	$6.4 \times 10^{35}$	$1.8 \times 10^{33}$	$5.5 \times 10^{41}$
9.3 % BA	First				273				$1.1 \times 10^{21}$
	Second	417	435	418	497	$1.3 \times 10^{34}$	$6.4 \times 10^{35}$	$3.6 \times 10^{34}$	$5.5 \times 10^{41}$

Abbreviations: DAP, diammonium phosphate; BA, boric acid; E, activation energy; A, pre-exponential factor.

The curvature is due to a smaller decrease in  $w$  (with increasing temperature) relative to the change in  $dw/dt$ . This in turn originates from the fact that the values of  $w$  used for the plots included an unknown amount of stable char which should be, but could not be, deducted. This must be borne in mind when these numbers are used.

The activation energies determined from the slopes of the linear portions of the plots and the pre-exponential factors determined from their intercepts are listed in Table I. As indicated above, these values are reported here without the corrections for the unknown weights of gasifiable material corresponding to the first and second reaction stages. The temperatures at which the weight loss switches from the first stage to the second stage in the Arrhenius plots were obtained from Figures 21–24 and are listed in Table II. These first and second reaction stages definitely correspond to the first, slow and second, rapid weight loss stages, respectively, as seen by comparison between the

 TABLE II  
 Temperature at Transfer from First Stage to Second Stage of Weight Loss

Treatment	O <sub>2</sub> %	Temperature (°C)			
		0	2.5	10	21
Untreated		322	312	308	302
2 % DAP		268	268	259	260
4.8 % DAP		242	249	237	241
10 % DAP		233	240	233	231
0.3 % BA				290	297
3.4 % BA					290
9.3 % BA					290



DTG curves in Figures 1 and 5, and the temperature values in Table II. Arrhenius parameters for the third stage (char oxidation) are not reported.

## DISCUSSION

### Effects of Ammonium Phosphate

The first stage of weight loss from cellulose has been interpreted to be caused by pyrolysis in the amorphous region,<sup>17-19</sup> and has been shown or inferred to give water in large amounts in addition to levoglucosan.<sup>17, 18, 20, 21</sup> The dehydration is accelerated by diammonium phosphate.<sup>22</sup> In other studies, DTA curves in an inert atmosphere of cellulose treated with mono- or diammonium phosphate have shown three or four endotherms.<sup>23-25</sup> Although only two endotherms can be detected in the present DSC results for nitrogen, it is inferred here that the first one is mainly caused by pyrolysis of the amorphous region, because the endotherm becomes deeper and shifts toward lower temperatures with an increase in the salt content, as shown in Figure 2. This first endotherm is masked in the oxidizing atmospheres, but the corresponding DTG shoulders are found and they behaved similarly even in the oxidizing atmospheres. Since the char yield increases with the salt content (except for the sample with a 10% salt content, in nitrogen), ammonium phosphate is seen here to simultaneously accelerate dehydration and char formation; these effects were previously shown by many authors.

Even though the char yield increases with salt content, the sharpness of the DSC exothermic peak, ascribed to oxidation of aliphatic groups in the char,<sup>15</sup> decreases with an increase in the salt content, as shown in Figures 6 and 7. This suggests that ammonium phosphate either inhibits oxidation or makes the char structure more stable.

In previous work, Arrhenius plots derived from TG results on the basis of an apparent first-order reaction have shown two stages of weight loss from cellulose both untreated and treated with flame retardants, in an inert atmosphere<sup>7, 26</sup> and air.<sup>7</sup> The activation energies were lower for the first low temperature stage than for the second stage; the present results are consistent with this. In this study the activation energies of both stages were reduced by diammonium phosphate treatment, agreeing with results for cellulose treated with ammonium dihydrogen phosphate by Tang;<sup>26</sup> here they decreased further with an increase in the salt content. A similar tendency for both of the activation energies has been shown by Kumagai and others<sup>7</sup> for filter paper and Avicel celluloses treated with phosphoric acid. Two weight loss stages for cellulose treated with ammonium dihydrogen phosphate were also found by Inagaki and Katsuura,<sup>27, 28</sup> though the order for the reactions was not unity. Also, both activation energies did not decrease with an increase in the salt content.

Reported values for the Arrhenius weight loss parameters are quite varied, depending on the kind and purity of the materials, atmosphere, heating procedure, and method of calculation. For example, Kumagai and others<sup>7</sup> have determined activation energies, respectively, ranging from 182 to 214 kJ/mol and 270 to 487 kJ/mol for the first and second weight loss stages, depending on the kind of cellulose and the atmosphere. On the other hand,

Tang's values<sup>26</sup> in vacuum are 146 and 234 kJ/mol for the first and second stages, respectively. Thus, the activation energies obtained here for untreated cellulose are in the range of reported values.

The main (second stage) weight loss from cellulose has been assumed to be driven by random chain-scission initiation and depropagation producing levoglucosan, and to be retarded by termination of the chain reaction;<sup>3,4</sup> this sequence is generally established for the thermal decomposition of many vinyl polymers. If the initiation process produces a radical because of asymmetry of the cellulose molecule about the glucosidic bond and if the termination mechanism, as previously proposed,<sup>4</sup> is grafting between an activated center on a chain fragment and a cellulose hydroxyl group, and, further, if the kinetic chain length is short, as estimated by Okamoto,<sup>3</sup> then the following rate equation applies at steady state:

$$\frac{d[R]}{dt} = \frac{k_i L}{V} - \frac{k_t \text{OH}_n R}{V^2} = 0 \quad (3)$$

where  $R$  is the number of radicals,  $t$  is the time,  $k_i$  and  $k_t$  the rate constants of the initiation and the termination reactions,  $L$  is the number of glucosidic linkages,  $\text{OH}_n$  is the number of hydroxyl groups, and  $V$  is the volume. The production rate of monomer, levoglucosan, is expressed as

$$\frac{dM}{dt} = k_p R \quad (4)$$

where  $M$  is the number of monomer units and  $k_p$  is the rate constant for the depropagation reaction. When the degree of polymerization (DP) is large compared to unity,  $L = n(\bar{p} - 1) \cong n\bar{p}$ , where  $n$  is the number of polymer molecules,  $\bar{p}$  is the number average DP, and also  $n\bar{p}$  is the total number of polymer structural units. Since the termination reaction does not significantly affect  $\text{OH}_n$ , which is equal to  $3n\bar{p}$ , one obtains

$$\frac{dM}{dt} = \left( \frac{k_p k_i}{3k_t} \right) V \quad (5)$$

from Eqs. (3) and (4) plus the preceding expressions.

We have no exact information on how  $V$  changes with the extent of pyrolysis in the solid state. If  $V$  is constant for a long time, the weight loss reaction order is zero. If, on the other hand the volume per structural unit,  $V_m$  is constant,  $V = V_m n\bar{p}$ ; then Eq. (5) reduces to

$$\frac{dM}{dt} = k_w n\bar{p} \quad (6)$$

where  $k_w = k_p k_i V_m / 3k_t$ , which is a first-order reaction. The second (rapid) weight loss stage in this study may be controlled by Eq. (6).

Ammonium phosphate accelerates the initiation, as shown by the lowering of the threshold temperature for weight loss, with increasing salt content and by previous results on DP measurements.<sup>29</sup> This salt, however also accelerates

the termination.<sup>29</sup> Since the overall activation energy of the second weight loss stage decreases with increasing salt content, the decrease in the activation energy for the initiation and/or depropagation is inferred here to be larger than the decrease in the termination value. Furthermore, since this salt accelerates the dehydration reaction especially during the first stage, thereby decreasing the available hydroxyl groups, the termination reaction is inhibited; therefore, the overall activation energy of the weight loss may decrease as well due to such modification of the hydroxyl groups.

The termination reaction, as well as the dehydration reaction, contributes to the char increase by formation of crosslinks. If, with increasing salt content, the depropagation rate becomes larger than the termination rate, the char yield will decline. This could explain the fact that the char yield in nitrogen is smaller from the sample with a 10% salt content than from that with a 4.8% salt content as shown in Figure 1.

### Effects of Boric Acid

The TG and DTG curves indicate that the beginning of weight loss and char formation are accelerated with an increase from 0 to 0.3% in boric acid; further acceleration is not apparent above this level of retardant. Since the sharpness of the first DSC exothermic peaks decreases with boric acid content and the peak temperature shifts upward with an increase above 0.3% as shown in Figure 20, boric acid evidently either inhibits oxidation or formation of the groups in the solid responsible for this exotherm (presumably aliphatic groups<sup>15</sup>).

There is no definite indication of low temperature shoulders on the DTG curves like those found for the samples treated with ammonium phosphate. This lack is reflected in the Arrhenius plots for the weight loss. The weight loss processes are not divided into two stages except in the highest oxygen concentration and for the sample with a 0.3% additive content in the 10% O<sub>2</sub> atmosphere. In these exceptions the first weight-loss stage is considerably shorter than that for the samples with ammonium phosphate. Therefore, boric acid is apparently acting here to suppress the first weight-loss stage.

Boric acid has previously been shown to have a lesser accelerating effect on the dehydration than other flame retardants<sup>22,30</sup> and it has also been found to cause the dehydration and rapid weight loss (depolymerization) reactions which occur simultaneously.<sup>22</sup> Furthermore, this retardant has been shown from DP measurements not only to promote random scission initiation, agreeing with the present accelerated onset of weight loss, but also to accelerate termination.<sup>12</sup> The observation that weight loss begins at a much higher temperature than that for the onset of random scission<sup>12</sup> may be explained by accelerated termination. The almost unchanging threshold temperature for weight loss seen in the TG curves of Figures 11, 14, and 15 implies that the cross-linked structures formed by the termination reaction have about the same stability as the original cellulose.

The overall activation energy of the weight loss increases somewhat with boric acid content, as seen in Table I. This agrees with previous kinetic analyses of TG<sup>22</sup> and isothermal heating<sup>31</sup> data for cellulose treated with boric acid. This increase in the activation energy may be due to both the accel-

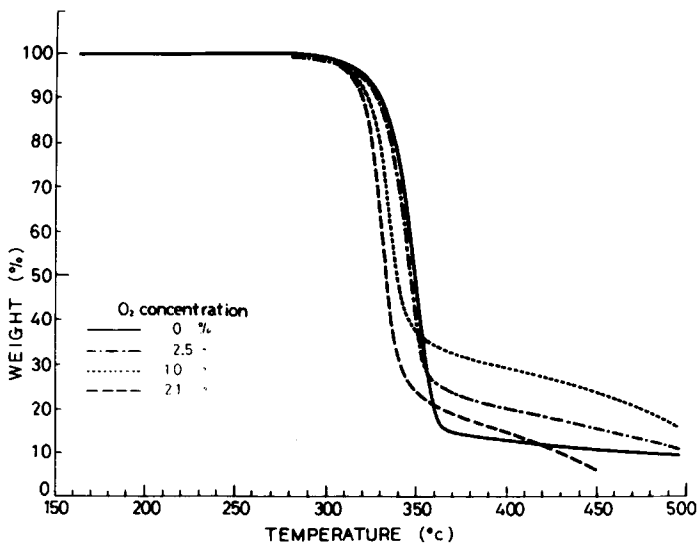


Fig. 25. TG curves of untreated cellulose in different  $O_2$  concentrations.

erated termination reaction and the cross-linked structures produced in the cellulose.

### Effect of Oxygen on the Pyrolysis

As stated above there are no simple monotonic effects of oxygen on the DTG results for samples with ammonium phosphate (see Figures 8 and 9) or on the DTG peak heights for samples with boric acid (see Figure 19). However, some interesting observations can be obtained from the TG curves when they are compared for the various oxygen concentrations, as shown in Figures 25–27. The char yield is not necessarily highest in a nitrogen atmosphere. However, as is generally expected, the char yield in nitrogen is higher than that in a 21% oxygen atmosphere (except for the untreated sample between 350 to 410°C in Figure 25). The beginning of the weight loss from untreated cellulose is accelerated with an increase in the oxygen concentration, but the onset of weight loss from samples with the 4.8% ammonium phosphate and 3.4% boric acid is retarded in a 2.5%  $O_2$  atmosphere compared to  $N_2$ , as shown in Figures 26 and 27.

In order to look into the oxygen effects on char formation, the char yields from each treated sample in the different atmospheres were obtained at the TG temperature at which the second stage (rapid) weight loss was completed in nitrogen. Although the exact values may be somewhat arbitrary, this determination will be enough to derive qualitative but consistent explanations of the oxygen effects. For the samples with ammonium phosphate, 10%  $O_2$  concentration gave the highest char yield for each retardant content (except for the 2.0 and 4.8% salt contents in nitrogen), as shown in Figure 28. For the samples with boric acid, again the same oxygen concentration produced the highest char yield for each retardant content, as shown in Figure 29. Although the effect of oxygen on char yield is not monotonic for all retardant concentrations, it is clear that an  $O_2$  concentration near 10% gives the highest char yield.

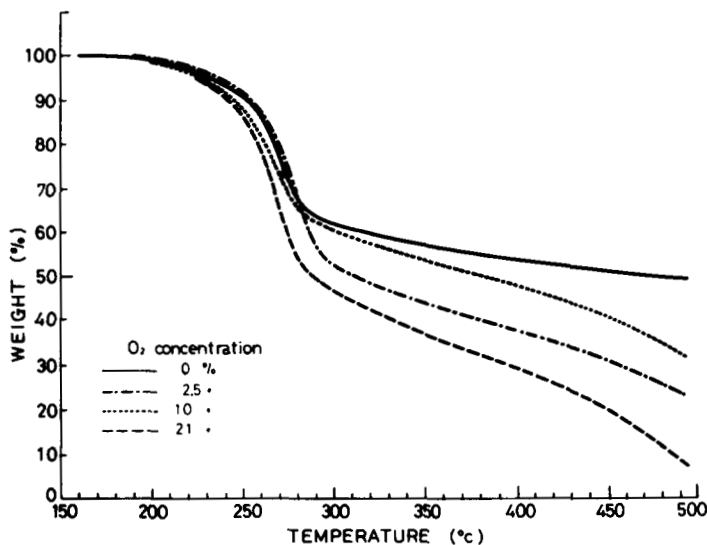


Fig. 26. TG curves in different O<sub>2</sub> concentrations of cellulose containing 4.8% ammonium phosphate.

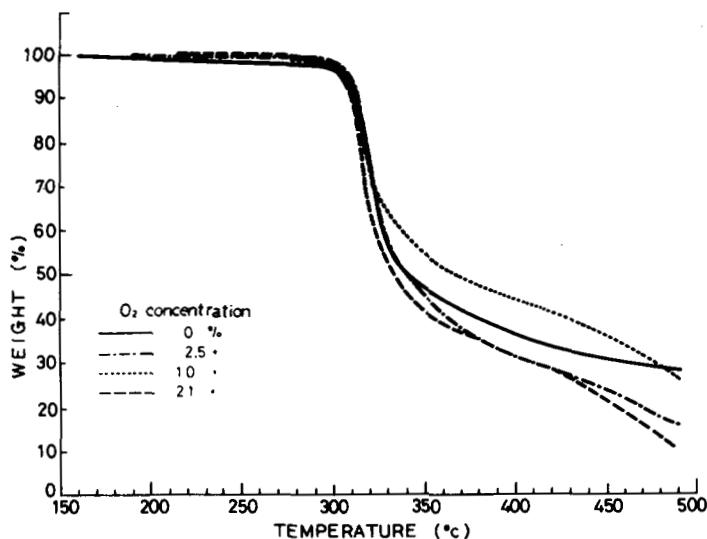


Fig. 27. TG curves in different O<sub>2</sub> concentrations of cellulose containing 3.4% boric acid.

For untreated cellulose, the activation energy of the first stage decreases with increasing oxygen concentration, as shown in Table I. This agrees with the acceleration of the beginning of the weight loss due to oxygen, as shown in Figure 25. The activation energy of the second stage increases with oxygen concentration. These tendencies, however, cannot be found for the treated samples. For ammonium phosphate-treated cellulose it seems that the activation energies of both of the stages did not change regardless of the oxygen concentration. For the sample with boric acid, on the other hand, the oxygen dependent change in the activation energy of the second stage looks inconsistent, though the values are the highest in 21% oxygen. The first weight loss

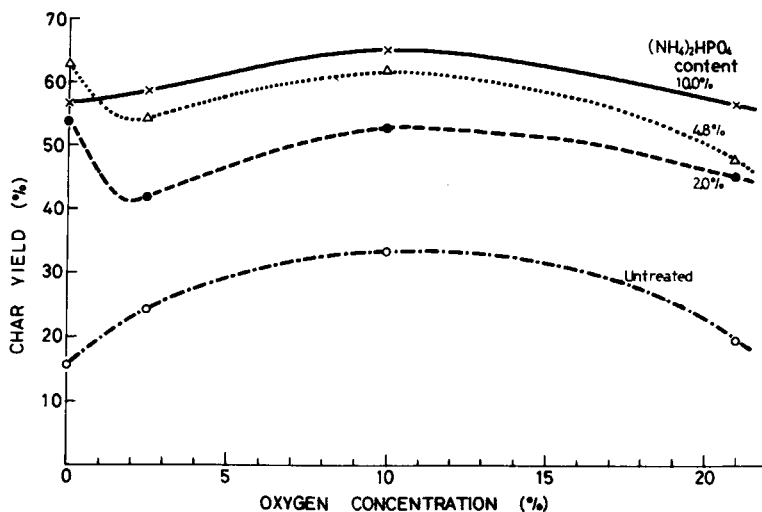


Fig. 28. Changes with  $\text{O}_2$  concentration in char yield for ammonium phosphate-treated cellulose (char yield determined at the temperature of the completion of the rapid weight loss in nitrogen).

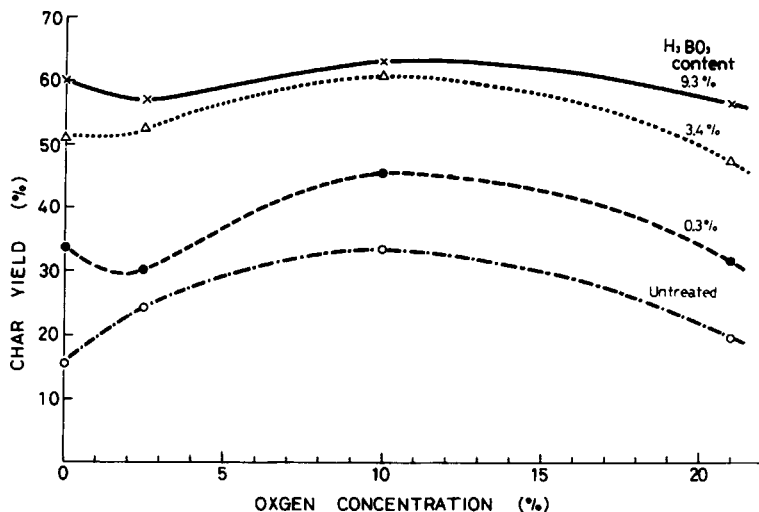


Fig. 29. Changes with  $\text{O}_2$  concentration in char yield for boric acid-treated cellulose (char yield determined at the temperature of the completion of the rapid weight loss in nitrogen).

stage in high oxygen concentrations for this sample may be caused by oxygen acceleration of the onset of weight loss.

Oxygen definitely plays three different roles in the pyrolysis, as seen from behaviors of the untreated sample. It accelerates the onset of weight loss (see Figure 25) and of crosslinking; it also exothermically gasifies the char, as shown by the DSC exotherm. Oxygen first accelerates random chain scission, probably through the formation of peroxides, as is generally accepted in polymer oxidation, and then promotes the onset of weight loss by oxidizing the cellulose, as interpreted by Shafizadeh and Bradbury.<sup>9</sup> These reactions probably occur preferentially in the amorphous region, as is suggested from

studies of the oxidation of polyethylene.<sup>32</sup> An activated center on a chain fragment may undergo accelerated termination by reacting with a peroxy radical to form a crosslink. Peroxide formation, as well as crosslink formation, makes the cellulose structure less ordered, and therefore the termination reactions are further accelerated due to the increase in the amount of the less ordered region. The increase in the activation energy of the second weight loss stage for untreated cellulose with increased oxygen may be due to such acceleration of the termination reactions and to the formation of cross-linked structures. The char yield increases with the extent of cross-linking but it then decreases due to the char gasification accelerated with an increase from 10 to 21% O<sub>2</sub>, as shown in Figures 28 and 29.

The oxygen effects are much reduced by the simultaneous retardant effects and the principal mechanism of oxygen action on the pyrolysis reactions seems different depending on the oxygen and retardant amounts. At a low concentration, such as 2.5%, oxygen may mainly accelerate scission of the glucosidic bond and of crosslinks preferentially formed by termination and dehydration due to the effect of the retardants. This reduces the char yield, as stated above. Nevertheless, with an increase in the oxygen concentration, the char yield increases, because peroxy and other radicals increase, thereby accelerating the cross-linking terminations. This explanation agrees with the finding that the activation energy of the second stage is the highest in 21% O<sub>2</sub> except for the sample with ammonium phosphate. Probably strong dehydration reaction due to ammonium phosphate makes the remaining cellulose structure too stable for the oxygen effect to be reflected in the Arrhenius parameters. Even in the high concentrations the oxygen effect to accelerate the scission of linkages is revealed by the occurrence of the first stage weight loss from cellulose with boric acid, whose dehydrating effect and therefore the stability of corresponding cellulose structure are smaller than those for ammonium phosphate.

It is concluded that, for samples treated with these flame retardants, oxygen accelerates random-scission initiation at low concentrations such as 2.5%, termination reactions at medium concentrations, and oxidation of the char at the highest concentrations, such as in air.

## CONCLUSIONS

As seen here and elsewhere, the weight-loss process from cellulose untreated and treated with flame retardants consists of three stages: a first, slow weight loss, a second, rapid weight loss, and a prolonged stage of char oxidation. The first two stages are accepted to follow an apparent first-order reaction. Here it is found that the main weight loss (second stage) may be explained by a model based on a chain reaction with random-scission initiation, depropagation producing levoglucosan, and grafting termination.

Diammonium phosphate accelerates the first two weight-loss stages and raises the char yield. Boric acid suppresses the first weight-loss stage and increases the char yield. These effects of the flame retardants are qualitatively explained here by a chain reaction mechanism in accord with the obtained Arrhenius parameters and char yields. Both of the retardants either accelerate the formation of stable char structures or inhibit the low temperature oxidation of the char.

The effects of oxygen on the pyrolysis are smaller than those of the retardants. Oxygen has three effects: it accelerates the beginning of the weight loss, it raises the char yield, and it promotes char oxidation. Oxygen either reduces or increases the effects of the retardants depending on its level. This ambivalent impact of oxygen in the presence of the retardants is qualitatively rationalized in accord with the proposed reaction mechanism.

For the future, it is desirable to establish a more precise model of the weight loss including the dehydration, because many flame retardants accelerate the production of water from cellulose.

The authors gratefully wish to acknowledge Dr. T. J. Ohlemiller of the National Bureau of Standards for his editorial help to their paper.

### References

1. P. K. Chatterjee and C. M. Conrad, *Text. Res. J.*, **36**, 487 (1966).
2. W. J. Parker and A. E. Lipska, U. S. Navy Radiological Defense Lab. Rept., USNRDL-TR-69 (1969).
3. H. Okamoto, *Mokuzai Gakkaishi*, **19**, 353 (1973).
4. T. Hirata, *Mokuzai Gakkaishi*, **22**, 238 (1976).
5. A. W. Bradbury, Y. Sakai, and F. Shafizadeh, *J. Appl. Polym. Sci.*, **23**, 371 (1979).
6. K. Kato and N. Takahashi, *Agr. Bio. Chem.*, **31**, 519 (1967).
7. Y. Kumagai, T. Ohuchi, C. Nagasawa, and M. Ono, *Mokuzai Gakkaishi*, **20**, 381 (1974).
8. C. Fairbridge, R. A. Ross, and S. P. Sood, *J. Appl. Polym. Sci.*, **22**, 497 (1978).
9. F. Shafizadeh and A. G. W. Bradbury, *J. Appl. Polym. Sci.*, **23**, 1431 (1979).
10. C. J. Hilado and C. J. Casey, *J. Fire Flamm.*, **10**, 140 (1979).
11. T. Hirata and H. Abe, *Mokuzai Gakkaishi*, **19**, 539 (1973).
12. T. Hirata, *Mokuzai Gakkaishi*, **27**, 125 (1981).
13. T. Hirata, *Bull. Forestry Forest Products Res. Inst.*, No. **304**, 77 (1979).
14. F. Shafizadeh, R. H. Furneaux, T. G. Cochran, J. P. Scholl, and Y. Sakai, *J. Appl. Polym. Sci.*, **23**, 3525 (1979).
15. Y. Sekiguchi and F. Shafizadeh, *J. Appl. Polym. Sci.*, **29**, 1267 (1984).
16. T. Hirata, *Pyrolysis of Cellulose, An Introduction to the Literature*, National Bureau of Standards, NBSIR 85-3218, August 1985.
17. O. P. Golova, A. M. Pakhomov, E. A. Andrievskaya, and R. G. Kryilova, *Dokl. Akad. Nauk SSSR*, **115**, 1122 (1957).
18. O. P. Golova and R. G. Kryilova, *Dokl. Akad. Nauk SSSR*, **116**, 3 (1957).
19. A. Basch and M. Lewin, *J. Polym. Sci., Polymer Chem. Ed.*, **12**, 2053 (1974).
20. S. L. Madorsky, V. E. Hart, and S. Straus, *J. Res. Natl. Bur. Stds.*, **56**, 2685 (1956).
21. T. Hirata and H. Okamoto, *J. Polym. Sci., Polymer Chem. Ed.*, **22**, 3071 (1984).
22. A. Nunomura, H. Ito, A. Kasai, and K. Komazawa, *Rept. Hokkaido Forest Products Res. Inst.*, No. **54**, 10 (1972).
23. K. Akita and M. Kase, *J. Polymer Sci.*, A-1, **5**, 833 (1967).
24. N. Inagaki and K. Katsuura, *J. Chem. Soc. Japan, Ind. Chem. Section*, **74**, 982 (1971).
25. T. Hirata and H. Abe, *Mokuzai Gakkaishi*, **19**, 483 (1973).
26. W. K. Tang, U. S. Forest Service Res. Paper, FPL 71 (1967).
27. N. Inagaki and K. Katsuura, *J. Chem. Soc. Japan, Ind. Chem. Section*, **72**, 2303 (1969).
28. N. Inagaki and K. Katsuura, *J. Chem. Soc. Japan, Ind. Chem. Section*, **73**, 1433 (1970).
29. T. Hirata, H. Okamoto, and K. Naito, *Mokuzai Gakkaishi*, **24**, 243 (1978).
30. F. H. Holmes and G. J. F. Shaw, *J. Appl. Chem.*, **11**, 210 (1961).
31. T. Hirata, *Mokuzai Gakkaishi*, **27**, 731 (1981).
32. J. P. Luongo, *J. Polym. Sci.*, B, **1**, 141 (1963).

Received July 3, 1986

Accepted September 9, 1986